BMC Oral Health

RESEARCH Open Access

Effect of E-glass fibers addition on compressive strength, flexural strength, hardness, and solubility of glass ionomer based cement

Tamer M. Hamdy[1*]

Abstract

Background In dentistry, glass-ionomer cements (GICs) are extensively used for a range of applications. The unique properties of GIC include fluoride ion release and recharge, chemical bonding to the tooth's hard tissues, biocompatibility, a thermal expansion coefficient like that of enamel and dentin, and acceptable aesthetics. Their high solubility and poor mechanical qualities are among their limitations. E-glass fibers are generally utilized to reinforce the polymer matrix and are identified by their higher silica content.

Objectives The purpose of the study was to assess the impact of adding (10 wt% and 20 wt%) silane-treated E-glass fibers to traditional GIC on its mechanical properties (compressive strength, flexural strength, and surface hardness) and solubility.

Methods The characterization of the E-glass fiber fillers was achieved by XRF, SEM, and PSD. The specimens were prepared by adding the E-glass fiber fillers to the traditional GIC at 10% and 20% by weight, forming two innovative groups, and compared with the unmodified GIC (control group). The physical properties (film thickness and initial setting time) were examined to confirm operability after mixing. The evaluation of the reinforced GIC was performed by assessing the compressive strength, flexural strength, hardness, and solubility ($n = 10$ specimens per test). A one-way ANOVA and Tukey tests were performed for statistical analysis ($p \leq 0.05$).

Results The traditional GIC showed the least compressive strength, flexural strength, hardness, and highest solubility. While the GIC reinforced with 20 wt% E-glass fibers showed the highest compressive strength, flexural strength, hardness, and least solubility. Meanwhile, GIC reinforced with 10 wt% showed intermediate results ($P \leq 0.05$).

Conclusion Using 20 wt% E-glass fiber as a filler with the traditional GIC provides a strengthening effect and reduced solubility.

Keywords Reinforcement, GIC, E-glass fibers, Compressive strength, Hardness, Solubility

*Correspondence:
Tamer M. Hamdy
tm.hamdy@nrc.sci.eg
[1]Restorative and Dental Materials Department, Oral and Dental Research Institute, National Research Centre (NRC), Giza, Dokki 12622, Egypt

Background

Polymers are commonly used in dentistry [1, 2]. The conservative dentistry procedures based on using adhesive restorative materials follow minimum tooth tissue removal while maintaining healthy tooth structure. Using restorative adhesive materials [3]. Glass ionomer cement (GIC) is a self-adhesive aesthetic restorative substance [4, 5]. Chemically, it is formed by an acid-base reaction. It is composed mainly of two components: weak polyacrylic acid and calcium fluoro-aluminosilicate glass fillers [6]. It has been used in many dental applications, including endodontic sealers, pit and fissure sealants, liner and bases, and minimally invasive and atraumatic direct restorative procedures [7].

GIC provides numerous benefits, including superior aesthetic qualities, fluoride release, chemical attachment to tooth structure, favorable thermal expansion, and biocompatibility [8, 9]. These materials have the ability to release and recharge fluoride over extended periods of time [10]. In the presence of calcium and phosphate ions, fluoride promotes the production of fluorapatite [10, 11]. When enough calcium and phosphate ions are present, it prevents the demineralization of enamel and dentin while encouraging remineralization at crystal surfaces. In early carious lesions, fluoride can prevent demineralization and encourage the remineralization of hard tooth tissues [11]. Furthermore, GIC has the capacity to release ions other than fluoride, such as calcium and aluminum; these ions promote the bioactivity and remineralization of enamel and dentin, mainly through the through the lactic acid buffering effect [12]. Even with these advantages, further improvement is required to overcome their drawbacks, which include their diminished mechanical properties and greater solubility rate. This could reduce their chances of longevity when they are used in regions that are subjected to high loads [13].Two critical physical attributes of a crucial component of restorative dentistry are film thickness and the dental cement's initial setting time, which give an indication of the workability of the cement [13].

The development of new polymeric structures and the use of inorganic fillers led to advancements in dental materials [14]. Surface treatment, grafting, and the addition of reinforcing fillers are examples of filler modifications that are successful in enhancing dental materials and extending their life span [15–18].

The objective of many studies was to enhance the mechanical properties of the GIC. This was achieved by incorporating various filler particles, such as metallic fillers such as titanium, silver, graphene, and carbon [19, 20], or bioactive fillers such as hydroxyapatite particles and bioactive glass [18, 21–24].

The majority of masticatory forces in the posterior region of the oral cavity are compressive [25–27]. Therefore, the most crucial mechanical characteristic of restorative materials is compressive strength. Restorative materials with inferior compressive strength are more likely to break [25, 26]. Compressive strength may be regarded as a crucial success indicator, as restorative materials with enhanced compressive strength can withstand masticatory and parafunctional stresses [28]. A material's flexural strength is a crucial characteristic that assesses the materials resistance to bending or fracturing under stresses [29]. Flexural strength is a suitable indicator of GIC strength since it reflects a clinical situation in which the restoration is being stressed by an opposing tooth [30]. It is an important aspect influencing how long any restoration lasts [31].

Nowadays, E-glass fiber reinforcement has emerged as an innovative and attractive approach in dentistry. It could provide an enhancement to the mechanical and physical qualities of dental materials by employing E-glass fibers in their composition. E-glass fibers have been the most frequently used fibers in dentistry due to their superior bonding with dental polymers and acceptable aesthetics [32].

A variety of variables, such as fiber diameter, length, orientation, percentage, and adhesion, affect the properties of fiber-reinforced materials [3]. Enhancing the mechanical qualities of the resulting structure requires improved adhesion between the fiber and matrix, which could be substantially improved by the silane treatment of the fiber [33, 34]. Therefore, the present study is intended to evaluate the impact of adding (10 wt% and 20 wt%) silane-treated E-glass fibers to traditional GIC on its compressive strength, surface hardness, and solubility and compared with the unmodified GIC (control group). The null hypothesis stated that the addition of E-glass fiber fillers to the traditional GIC at 10% and 20% by weight has no influence on the compressive strength, flexural strength, hardness, or solubility in comparison to the untreated control group.

Methods

The present experimental study was approved by the Medical Research Ethical Committee (MREC) of the National Research Centre (NRC), Cairo, Egypt (reference number: 305,032,023). For this study, a commercially conventional chemically cured GIC was utilized in powder and liquid form: Fuji IX GP Extra (GC Corporation, Tokyo, Japan). Commercial E-glass fiber powder was used as a filler (Fibertec Inc., Scotland Boulevard, Bridgewater, MA, U.S.A.). The details of the materials used in the current study are listed in Table (1).

Table 1 The detailed data on the used materials in the study

Material	Manufacturer	Composition	Batch number
Fuji IX GP Extra	GC Corporation, Tokyo, Japan.	Polyacrylic acid, fluoro-alumino-silicate glass, other ingredients.	002578
Microglass Milled Fiber 9110 Series	Fibertec Inc., Scotland Boulevard, Bridgewater, MA, U.S.A.	Silane treated E-glass fiber, consists of highly transparent high aspect ratio E-glass fiberglass, 16 µm diameter, 150 µm length. SiO_2 (50–55 wt%), CaO (20–24 wt%), MgO (20–24 wt%), B_2O_3 (1–3 wt%), Al_2O_3 (4- 6wt%).	030095

Chemical and morphologic characterization of E-glass powder

X-ray fluorescence (XRF) analysis

The qualitative chemical analysis of the E-glass powder was carried out by non-destructive XRF analysis (X-MET3000TXR, Oxford Instruments GmbH Co., Borsigstrasse, Germany) to verify the chemical composition of the used fillers [35]. The instrument examination was performed at 40 kV, 40 mA, and 1600 W.

Scanning electron microscope (SEM)

The morphological analysis of the E-glass shape and distribution were examined via scanning electron microscopy (SEM) (Quanta 250 FEG, FEI Company, Hillsboro, OR, USA). It was carried out with an accelerating voltage range of 20.0 kV to 30.0 kV, and the magnification was 1600X. The E-glass fibers were examined before mixing as well as after mixing with the GIC.

Particle size distribution (PSD) analysis

The particle size of E-glass fiber fillers was examined using a particle size analyzer with a NICOMP 380 ZLS dynamic light scattering (DLS) instrument (PSS Nicomp 380 particle sizer, Santa Barbara, California, USA). The PSD of the E-glass particles was investigated. Based on histogram analysis, the average particle diameter of E-glass fiber particles was provided. The Gaussian particle size distributions and NICOMP distribution curves were determined.

Physical characterization of the mix

Film thickness and setting time measurements were used to evaluate the physical characteristics of the control and treated specimens. Following the guidelines of ISO standard 9917-2 from the International Standard Organization (ISO), the film thickness of the control and treated specimens was examined [36]. Four measurements were made of the thickness of two flat glass plates that were connected together, to the nearest 0.1 m, using an electronic digital caliper (Digital Vernier Calliper, Mitutoyo, Japan). A record of this reading was made (reading A). According to the manufacturer's directions, the cement for each group ($n=10$) was mixed. Following mixing, each cement mixture was equally divided between the two glass plates. The upper glass plate was subjected to a load of 147 N using a universal testing apparatus (Shimadzu Autograph AG-X Plus, Kyoto, Japan). After seven minutes, the total thickness of the plates with the specimen in between was noted as reading B. The difference between the thickness of the plates with and without the material between (B-A) was used to calculate the final total film thickness for the specimen being tested [36].

The Gillmore needles (Humboldt MFG., Norridge, IL, USA) were used to determine the initial setting times in accordance with ADA guidelines [37]. A light needle weighing 113.4 g and having a tip diameter of 2.12 mm was used to calculate the initial setup time. The needle was positioned on the surface every 30 s. The initial setting times were calculated starting from the point at which mixing began and ending when the needle left no surface marks, respectively. For every group, ten samples were measured [38].

Sample size calculation

The sample size calculation was based on a similar study [3, 30]. With an alpha level of 0.05 and a power of 85%, a sample size was determined using G*Power software version 3.1.9.7 (Heinrich Heine University Duesseldorf, Duesseldorf, Germany). The minimum sample size needed with this effect size is ($n=10$ per group) to test compressive strength, flexural strength, microhardness, and solubility.

Study design

A total of 120 specimens were prepared according to each type of the analytic test. They were standardized and evenly distributed in three groups of 40 specimens. These were divided into three subgroups of specimens ($n=10$) for examination of compressive strength, flexural stregth, microhardness, and solubility, as represented in Fig. 1.

Sample preparation

The preparation of the control group was done by mixing the conventional GIC powder with their liquid. While the reinforced groups were obtained by mixing 10 wt% and 20 wt% E-glass fiber powder, respectively, with the conventional GIC powder, using an amalgamator, to reach a homogenous powder mixture. The prepared powder was then mixed with the GIC liquid. The mixing of powder and liquid was done according to the manufacturer's instructions. The mixed material from each group was then filled into specially designed molds according to the test specifications.

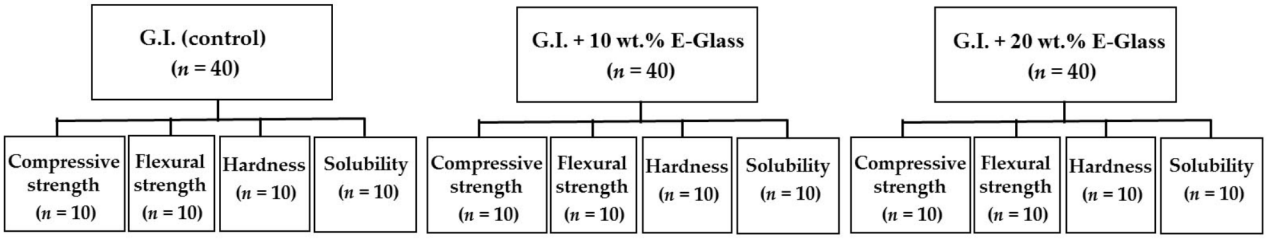

Fig. 1 Distribution of groups according to materials and types of tests

Analytic tests

Compressive strength test

In accordance with ISO standards 9917-2:2017 for water-based cements, compressive strength was assessed for each group [39]. Ten cylindrical specimens (n=10) were created for each group using a split Teflon mold with internal dimensions (measuring 6±0.1 mm in height and 4±0.1 mm in diameter). The cement paste was loaded into the mold with a syringe. The top and bottom surfaces of the surface were covered with a celluloid strip and glass slide. The specimens were stored at 37 °C and a relative humidity of 100% for 60 min. and were carefully removed from the molds, then stored for 23 h at 37 °C in deionized water. The excess cement was eliminated by polishing both sides with 500-grit carbide paper under water irrigation on a grinder-polisher (Buehler, IL, USA) to reach the proper dimensions of 4 mm in diameter and 6 mm in height. Compressive strength tests were performed using a universal testing machine (Shimadzu Autograph AG-X plus 5 kN, Kyoto, Japan) with a crosshead speed of 1 mm/min. Specimens were loaded in compression until a fracture occurred. The compressive strength was determined in MPa using the following formula [39]:

Compression strength = $\frac{4P}{\pi d^2}$

Where: P is the fracture load (N); d is the diameter (mm).

Flexural strength test

In accordance with ISO 20795-1, a flexural strength test was assessed utilizing 3-point bending [40]. . Specimens measuring 64 mm in length, 10 mm in width, and 3.3 mm in thickness were created using a metallic mold [40]. . A universal testing machine (Model 3345; Instron Industrial Products, Norwood, MA, USA) was used to evaluate the specimens. Using a load cell of 500 N, the load was delivered to the center of the specimens, which were maintained over a 2-point support span of 50 mm apart and a crosshead speed of 5 mm/min. Until they broke, the specimens were loaded. In Newtons (N), the load at fracture was expressed. The following formula was used to compute the flexural strength (FS) in MPa [41, 42]. : $FS=3PL/2bh^2$. Where (L) is the distance between the supports (mm); (b) is the breadth (mm); (h) is the height of the specimen (mm); and (P) is the maximum load at fracture (N).

Vickers hardness (VH) test

Ten disc-shaped specimens (n=10) per group measuring 5 mm in height and 2 mm in diameter were prepared using Teflon mold [3]. The hardened specimens were removed from the molds and subsequently immersed in distilled water and maintained at 37 °C for 24 h in a highly humid incubator. After 24 h, the specimens were removed from the solution and dried. Surface microhardness for each specimen was determined using a digital Vickers hardness tester (NEXUS 400TM, INNOVATEST, model no. 4503, Maastricht, Netherlands). The indentations were made within 10 s of dwell time at a load of 100 g at 40 x magnificence. The results were expressed in Vickers hardness numbers (VHN) automatically using the formula [3]:

$VHN=1.8544\ P/d^2$, where (p) is the applied force in kilograms and (d) is the mean of the two diagonals gained from the indentation in mm.

Each specimen was indented three times and averaged to calculate the mean Vickers microhardness values (VHN).

Solubility percentage test

Solubility was tested using a Teflon mold that measured 7 mm in diameter and 2 mm in thickness, producing a disc-shaped specimen (n=10) [43]. Every group's specimens were kept for two hours in a desiccator filled with silica gel (Merck KGaA, Darmstadt, Germany), and then for a further twenty-two hours, they were incubated at 37 °C. First mass (M1) values were obtained by weighing specimens with an accuracy of 0.001 g on a precision analytical balance (Adam Equipment 4 digits precision weighing balance, Adam Equipment Inc., Oxford, UK). The samples were then kept for seven days and incubated at 37 °C for seven days after being submerged in a plastic flask filled with 25 mL of distilled water. To obtain the mass values of the specimens after immersion (M2), each specimen was then taken out and carefully dried with

Table 2 Chemical compositions (wt%) of E-glass determined by XRF analysis

Chemical composition	wt%
SiO_2	53
Al_2O_3	4
B_2O_3	1
MgO	20
CaO	21
K_2O	1

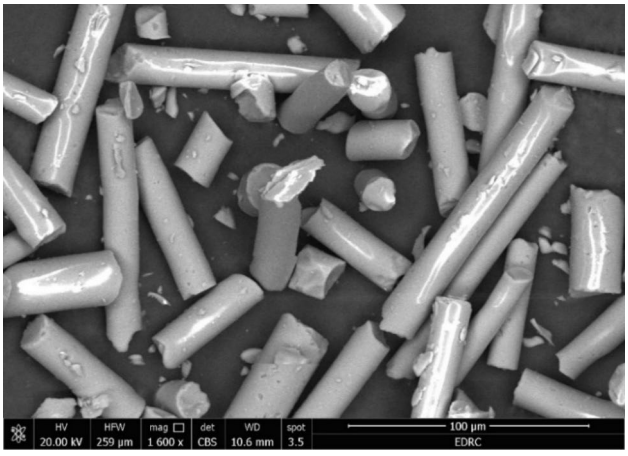

Fig. 2 SEM image of E-glass fibers

absorbent paper [44]. Using the equation, the percentage of solubility was determined [45]:

$$(M1 - M2)/M1 \times 100\%$$

where M1 is the initial mass and M2 is the final mass of the specimens. The test was repeated three times [43].

Statistical analysis

The Statistical Package for the Social Sciences (SPSS) 16.0 statistical program (IBM-SPSS version 27.0, New York, NY, USA) was used to conduct the statistical study. Using the Kolmogrov-Smirnov and Shapiro-Wilk tests, the data revealed a normal distribution. Analysis of Variance (ANOVA) and Tukey tests were utilized to compare the mean film thickness (µm), initial setting time (seconds), compressive strength (MPa), flexural strength (MPa), hardness (VHN), and solubility (%) for the glass ionomer (control), G.I. reinforced with 10 wt% E-glass, and G.I. reinforced with 20 wt% E-glass. The significance level was set at $P \leq 0.05$.

Results

XRF characterization results

The chemical composition of E-glass powder analyzed by XRF is shown in Table (2). The XRF results revealed that SiO_2 constituted most of the fibers, which weighed about 53 wt%. MgO and CaO contents were 20 and 21 wt%, respectively. The Al_2O_3 concentration was 4 wt%. There was 1 wt% of K_2O, and 1 wt% of B_2O_3.

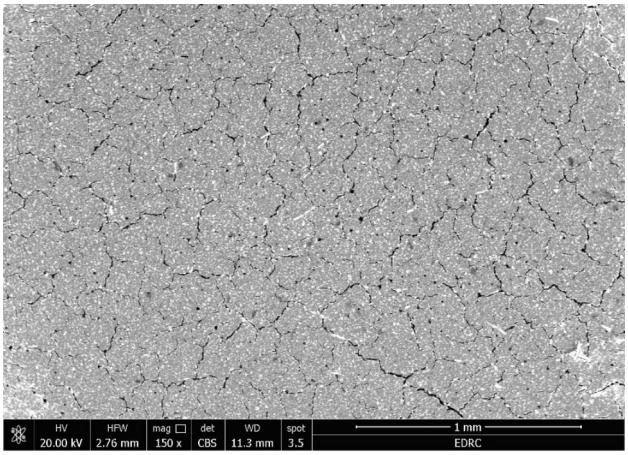

Fig. 3 SEM image after mixing of 10 wt% E-glass fibers with GIC at 150 X magnification

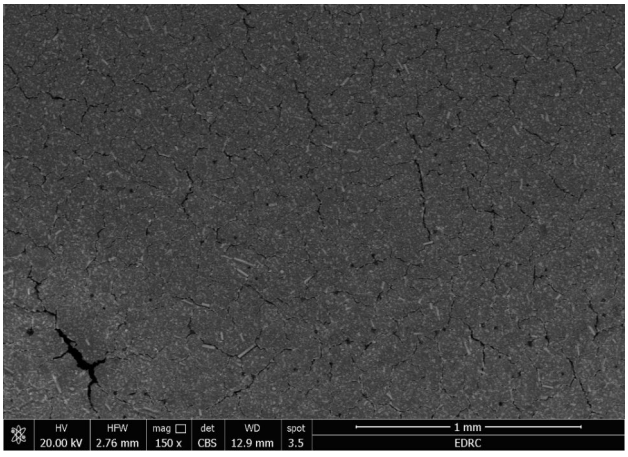

Fig. 4 SEM image after mixing of 20 wt% E-glass fibers with GIC at 150 X magnification

SEM characterization results

As seen in Fig. 2, the SEM micrograph of the E-glass fibers was acquired at a magnification of 1600 X. The SEM scans showed a short, homogeneous, straight filament morphology. Furthermore, the fibers had a smooth and shiny surface and were uniformly dispersed.

As shown in Figs. (3, 4, 5 and 6), the SEM micrograph of the E-glass fibers (10 wt% and 20 wt%) after mixing with GIC E-glass was acquired at a magnification of 150 X and 1000 X. The SEM scans showed a uniform distribution of the short glass fibers in both 10 wt% and 20 wt% concentrations. Moreover, the bonding between glass fibers and GIC appears to be tight. Furthermore, some cracks were exhibited on the surface of GIC.

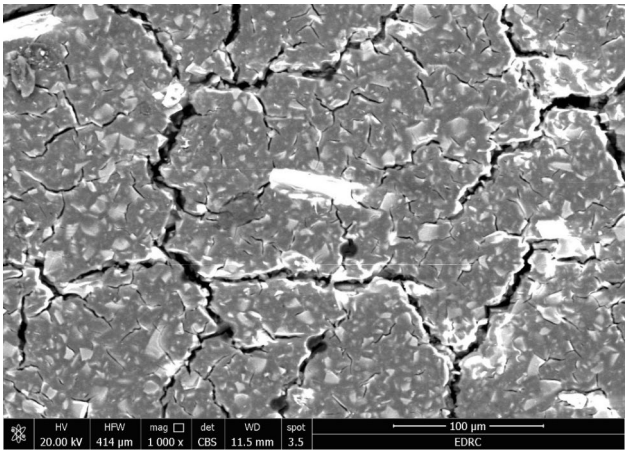

Fig. 5 SEM image after mixing of 10 wt% E-glass fibers with GIC at 1000 X magnification

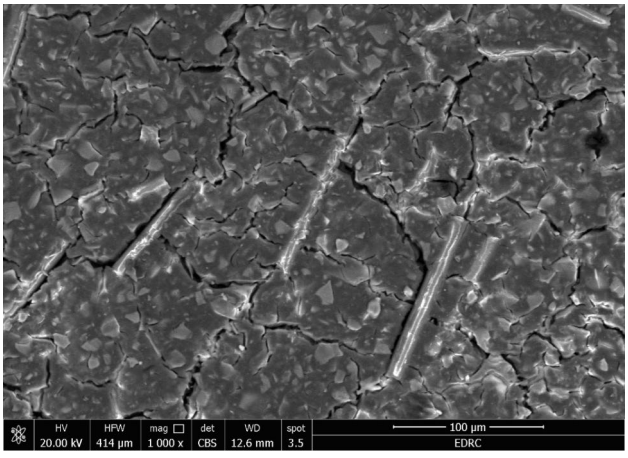

Fig. 6 SEM image after mixing of 20 wt% E-glass fibers with GIC at 1000 X magnification

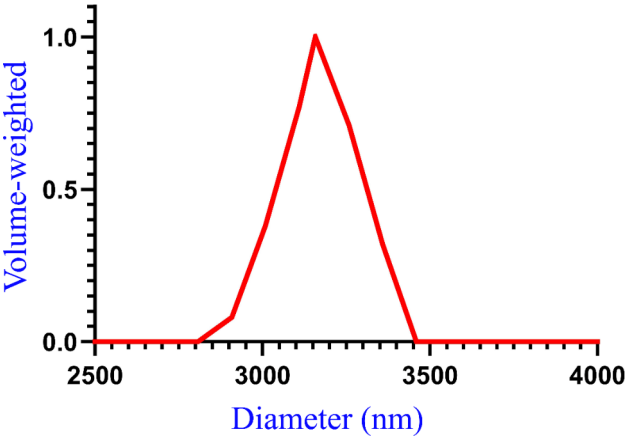

Fig. 7 E-glass fibers diameter distribution

Table 3 The film thickness mean and standard deviation values among the groups (µm)

Test	GIC (control)	GIC reinforced with 10 wt% E-glass	GIC reinforced with 20 wt% E-glass	*P* value
Film thickness (µm)	22.4 ± 1.1	23.4 ± 0.5	23.8 ± 0.8	0.7

Table 4 The initial setting time mean and standard deviation values among the groups (seconds)

Test	GIC (control)	GIC reinforced with 10 wt% E-glass	GIC reinforced with 20 wt% E-glass	*P* value
initial setting time (seconds)	98.8 ± 1.9	100.6 ± 0.5	100.8 ± 1	0.1*

Particle size characterization results

The diameter distribution of the E-glass fibers analyzed by DSL is plotted in Fig. 7. The diameter distribution of the E-glass fibers according to Gaussian distribution analysis can be summarized as follows: The intensity-weighted Gaussian distribution mean diameter was 1.1307 µm, and the volume-weighted Gaussian distribution mean diameter was 3.1579 µm. In addition, the mean length distribution was 315.79 µm. Moreover, the mean aspect ratio was 100.

Physical characterization results

Film thickness

Table 3 displays the film thickness data for the control and reinforced specimens. There was no significant difference ($P=0.7$) in the film thickness values between the untreated GIC (control) group (22.4 µm) and the GIC reinforced with 10 wt% and 20 wt% E-glass groups (23.4 µm and 23.8 µm, respectively).

Setting time

Table 4 shows the control and reinforced specimens' initial setting time results. There was no significant difference ($P=0.1$) in the initial setting time between the untreated GIC (control) group (98.8 s) and the GIC reinforced with 10 wt% and 20 wt% E-glass groups (100.6 and 100.8 s, respectively).

Analytical test results

Compressive strength results

Table 5 presents the results of the compressive strength. The mean values of the three groups varied significantly from each other. The GIC (control) showed the least compressive strength (96 MPa), While the GIC reinforced with 20 wt% E-glass showed the highest compressive strength (136 MPa), Meanwhile, GIC reinforced

Table 5 The compressive strength mean and standard deviation values among the groups (MPa)

Test	GIC (control)	GIC reinforced with 10 wt% E-glass	GIC reinforced with 20 wt% E-glass	*P* value
Compressive strength (MPa)	$96^{a} \pm 3.2$	$115.2^{b} \pm 3.3$	$136^{c} \pm 4$	0.00001*

Different small letters in the same row are significant difference, * denotes significant difference as $P \leq 0.05$

Table 6 The flexural strength mean and standard deviation values among the groups (MPa)

Test	GIC (control)	GIC reinforced with 10 wt% E-glass	GIC reinforced with 20 wt% E-glass	*P* value
Flexural strength (MPa)	$47^{a} \pm 1.6$	$57.2^{b} \pm 1.3$	$67.4^{c} \pm 1.1$	0.0001*

Different small letters in the same row are significant difference, * denotes significant difference as $P \leq 0.05$

Table 7 The hardness mean and standard deviation values among the groups (VHN)

Test	GIC (control)	GIC reinforced with 10 wt% E-glass	GIC reinforced with 20 wt% E-glass	*P* value
Hardness (VHN)	$44.4^{a} \pm 0.6$	$58.8^{b} \pm 1.4$	$75.9^{c} \pm 3.5$	0.00001*

Different small letters in the same row are significant difference, * denotes significant difference as $P \leq 0.05$

with 10 wt% showed intermediate results (115.2 MPa), ($P=0.0001$*).

Flexural strength results

Table 6 shows the results of the flexural strength. The mean values of the three groups varied significantly from each other. The GIC (control) showed the least flexural strength (47 MPa), while the GIC reinforced with 20 wt% E-glass showed the highest flexural strength (76.4 MPa). Meanwhile, the GIC reinforced with 10 wt% showed intermediate results (57.2 MPa), ($P=0.0001$*).

Hardness results

Table 7 presents the results of the surface hardness. The mean values of the three groups varied significantly from each other. The GIC (control) showed the least hardness (44.4 VHN), While the GIC reinforced with 20 wt% E-glass showed the highest hardness (75.9 VHN), Meanwhile, GIC reinforced with 10 wt% showed intermediate results (58.8 VHN), ($P=0.0001$*).

Table 8 The solubility mean and standard deviation values among the groups (%)

Test	GIC (control)	GIC reinforced with 10 wt% E-glass	GIC reinforced with 20 wt% E-glass	*P* value
Solubility (%)	$5.5^{c} \pm 0.3$	$3.2^{b} \pm 0.2$	$1.07^{a} \pm 0.05$	0.00001*

Different small letters in the same row are significant difference, * denotes significant difference as $P \leq 0.05$

Solubility results

Table 8 presents the results of the surface solubility. The mean values of the three groups varied significantly from each other. The GIC (control) showed the highest solubility (5.5%). While the GIC reinforced with 20 wt% E-glass showed and least solubility (1.07%). Meanwhile, GIC reinforced with 10 wt% showed intermediate results (3.2%), ($P=0.0001$*).

Discussion

Traditional GICs are used widely in dentistry because of their distinctive characteristics, including their chemical adhesion to tooth structures, which require minimal dental preparation, the ability to release fluoride, biological computability, and thermal computability with enamel, all of which reduce the amount of tooth preparation needed [46]. However, one of the primary challenges with GICs is their inferior mechanical features [47]. Since most mastication forces are compressive, a compressive strength test resembles the load applied to materials used in dental treatment [48]. Moreover, the compressive strength of GIC is commonly measured after 24 h wet storage [49]. Both compressive and flexural analysis were employed to mimic the stress placed on the materials used in clinical dentistry.

The durability of the restorations greatly depends on the resistance of the restorative material to intraoral circumstances. When dental materials are exposed to the oral environment for extended periods of time, the contact may cause the surface layers to dissolve or deteriorate [50]. Solubility and surface hardness are important features that determine the longevity of the GIC [51]. Furthermore, the material's clinical durability is significantly influenced by its flexural strength [22]. The ideal' dental cement and restoration should have several features, such as high surface and mechanical characteristics, adequate setting time, and a low film thickness (less than 25 μm) for the luting agent [52].

There have been several attempts to improve the mechanical properties of the GICs by incorporating reinforcement filler [53]. High aspect ratio E-glass fibers reinforcement is used in dentistry as well as numerous other technical fields. However, they haven't been thoroughly investigated with GICs [3].

The adhesion between the fibers and matrix has an important influence on the mechanical properties of the material [54]. To ensure that the load gets transferred to the stronger fibers, adequate adhesion between the fiber and matrix is necessary to ensure proper load transfer [54]. Therefore, the selected E-glass fibers were silane-treated in order to improve the adhesion of the fillers [33, 34].

The current study used two concentrations of E-glass fibers: 10 wt% and 20 wt%. According to a previous investigation, the strength of the restoration was reduced when fibers loading exceeded 25 wt% [54], which may be attributed to the fact that excessive fiber loading may create microstructural voids or flaws [54]. These microstructural flaws may have a determinate effect on the compressive strength and surface microhardness. Moreover, it may increase the solubility of the GIC [55].

This study was done to evaluate the effects of incorporating (10 wt% and 20 wt%) silane-treated E-glass fibers into conventional GIC on their compressive strength, flexural strength, hardness, and solubility. The results indicated that incorporation of E-glass fibers would enhance the mechanical performance of conventional GIC with an increase in compressive strength, flexural strength, surface hardness, and reduction in solubility compared to conventional GIC. The incorporation of a concentration of 20 wt% E-glass fibers provides a more favorable result than that of 10 wt%. Therefore, the null hypothesis of this study was rejected.

The chemical composition of the fibers was confirmed by X-ray spectrometry. The XRD data showed that the primary constituents of the E-glass fibers were SiO_2, Al_2O_3, MgO, and CaO, with small amounts of B_2O_3 and K_2O. The results were consistent with the chemical content of the frequently utilized E-glass reinforcing fibers [56].

SEM imaging is an ideal method for analyzing the uniformity and homogeneity of glass fiber distribution [57]. The distribution, orientation, aspect ratio, and morphology of the fibers could be identified by the SEM examination [58]. The SEM image results of the reinforced fibers show a short and thin fiber structure which may be crucial for the possible strengthening effects. Moreover, the SEM image results after mixing the reinforced groups showed a nearly uniform distribution of a short E-glass fibers within the GIC, which denotes good incorporation of the E-glass fibers during the mixing procedure. Furthermore, there seems to be a tight bond between the E-glass fibers and the GIC, which may be attributed to the silane treatment of the E-glass fibers [33, 34], This indicates that the addition of E-glass fiber increases the GIC's strength. On the other hand, some cracks exhibited on the surface of GIC may be due to dehydration during specimen preparation [11, 59]. The cracks noticed on the matrix surface may also be caused by the attack of freeze-dried acid polymers on the basic glass powder [60].

Particle size and distribution analysis are precise and essential techniques for enhancing the use of filler particles. It is believed to provide an accurate method for measuring the size of the particles [61]. Combining the diameter, length, and aspect ratio distribution data from the particle size analysis indicate a short glass fiber with a high aspect ratio, which may be crucial factors in determining the reinforcement potential of E-glass fibers [62].

Dental cement should have a film thickness of no more than 25 μm for water-based luting cements, in compliance with ADA No. 8 [63]. Enhanced marginal adaptation and improved restoration retention are the results of minimal film thickness of the dental cements [64]. Physical characterization results showed a film thickness of less than 25 μm is provided by both the treated and control groups with no significant difference between the them. Regarding the initial setting time, there was also no significant difference between the groups. These findings may be explained by the lower concentration of the incorporated short fibers.

The results of the compressive strength investigation showed that the modified groups, through the incorporation of E-glass fiber fillers into conventional GIC, significantly improved the compressive strength compared to the unmodified groups. This result could be explained by the predicted strengthening effect of the fillers made of E-glass fibers [32, 65]. The reinforcement effect may be due to the high rigidity of the E-glass fibers, which act as a crack stopper that prevents cracks from starting and spreading [3]. As a result, the material gains increased fracture resistance [66].

The improvement of the compressive strength in the group modified by the incorporation of 20 wt% E-glass fibers was more pronounced than that modified by the incorporation of only 10 wt% E-glass fibers. This may be attributed to the higher concentration of fibers, which provide a stronger effect [3, 67]. These findings come in agreement with the study provided by Sari et al. [3].

All of the reinforced groups in this study show an increase in flexural strength rather than the control group; this may be due to the adequate impregnation and bonding of silane-treated fibers to the GIC, which may prevent crack propagation by exerting a force opposing the crack [68]. Moreover, the maximum flexural strength was obtained by impregnation of E-glass fiber with GIC having a concentration of 20 wt%; this may be attributed to the increase in the reinforcing effect of the impregnated fibers [69].

The results of the surface hardness examination showed that the GIC reinforced with 20 wt% E-glass showed the highest hardness. While GIC reinforced with 10 wt% showed intermediate results, the unmodified

GIC showed the least hardness. These results could be explained by the hard E-glass fiber filler phase that exists within the matrix and acts as the strongest reinforcement [70, 71].

In the present study, the GIC modified with 10 wt% and 20 wt% E-glass fiber addition reduced the solubility more than the unmodified GIC. The low solubility of the integrated E-glass fibers could potentially explain this finding [72, 73].

Other studies were conducted to improve the mechanical properties of the GIC. Murugan et al. [74], aim to improve the mechanical properties of the GIC by incorporating nanohydroxyapatite. They found that the reinforced GIC displayed increased compressive strength and fracture toughness and decreased cytotoxicity and microleakage. Beketova et al. [75], examined the effects of adding zirconia nano-fillers to GIC. They found that such an addition significantly improved the flexural strength and bond strength, decreasing water sorption without negatively affecting the film thickness. Moreover, Abed et al. [76], revealed that the addition of 4 wt% silver nanoparticles preserves the same bond quality as GIC while improving the mechanical characteristics. Furthermore, Chaudhary et al. [77]. Evaluated the effect of the addition of 3 wt% titanium dioxide nano powder and 10 wt% nanohydroxyapatite to GIC. The results showed that the GIC modified with titanium dioxide showed the highest flexural and compressive strength.

One of the study's limitations is that the experimental conditions weren't exactly like the clinical ones. Moreover, the release of the fluoride ions was not examined after the addition of E-glass fibers. Additionally, the study investigated the mechanical properties in only short-term storage time. It is suggested that more research be done to examine the potential impacts of adding E-glass fibers to GIC at varying aspect ratios, fiber orientations, and amounts. Moreover, it is recommended to do a further study to assess the surface roughness, Further studies are recommended to investigate the mechanical properties after prolonged soaking. Moreover, it is recommended to examine the remineralization potential after the incorporation of E-glass fibers.

Conclusions

Compared to traditional GIC dental cement, the innovatively reinforced GIC with 20 wt% silane-treated E-glass fiber fillers offer improved compressive strength, flexural strength, hardness, and decreased solubility. As a result, it may be utilized as an alternative.

Abbreviations

GICs	Glass ionomer cements
wt.%	Weight%
MREC	Medical Research Ethical Committee
NRC	National Research Centre
XRF	X-ray fluorescence
SEM	Scanning electron microscope
PSD	Particle size distribution
DLS	Dynamic light scattering
ISO	International Organization for Standardization
MPa	Megapascal
VH	Vickers microhardness
VHN	Vickers hardness numbers

Acknowledgements

Not applicable.

Author contributions

T. M. H. contributed to the conception and design of the study, collection of data, interpretation of the analyzed data, checked the data and results, writing the manuscript, revised and reviewed the draft manuscript, read and approved the manuscript.

Funding

Open access funding provided by The Science, Technology & Innovation Funding Authority (STDF) in cooperation with The Egyptian Knowledge Bank (EKB).

Data availability

The data that support the findings of this study are available from the corresponding author upon reasonable request.

Declarations

Ethics approval and consent to participate

This study received ethical approval from the Medical Research Ethical Committee (MREC) of National Research Centre (NRC); Cairo, Egypt (reference number: 305032023). All methods were performed in accordance with the Declaration of Helsinki.

Consent for publication

Not applicable.

Competing interests

The authors declare that they have no competing interests.

Received: 14 April 2024 / Accepted: 5 June 2024
Published online: 27 June 2024

References

1. Abdelraouf RM. Chemical analysis and microstructure examination of extended-pour alginate impression versus conventional one (characterization of dental extended-pour alginate). Int J Polym Mater Polym Biomater. 2018. https://doi.org/10.1080/00914037.2017.1362636.
2. Abdelraouf RM, Mohammed M, Abdelgawad F. Evaluation of shear-bond-strength of dental self-adhering flowable resin-composite versus total-etch one to enamel and dentin surfaces: an in-vitro study. Open Access Maced J Med Sci. 2019;7:2162–6.
3. Sari F, Ugurlu M. Reinforcement of resin-modified glass-ionomer cement with glass fiber and graphene oxide. J Mech Behav Biomed Mater. 2023;142.
4. Torres C, Ávila D, Gonçalves LL, Meirelles L, Mailart MC, Di Nicoló R, et al. Glass Ionomer Versus Self-adhesive cement and the clinical performance of Zirconia Coping/Press-on Porcelain crowns. Oper Dent. 2021. https://doi.org/10.2341/20-229-C.
5. Hamdy TM. Interfacial microscopic examination and chemical analysis of resin-dentin interface of self-adhering flowable resin composite. F1000Research. 2017;6:1688.
6. Kampanas N-S, Antoniadou M. Glass Ionomer cements for the restoration of non-carious cervical lesions in the geriatric patient. J Funct Biomater. 2018;9:1–9.
7. Sidhu S, Nicholson J. A review of Glass-Ionomer cements for Clinical Dentistry. J Funct Biomater. 2016;7:16.

8. Moghimi M, Jafarpour D, Ferooz R, Bagheri R. Protective effect of a nanofilled resin-based coating on wear resistance of glass ionomer cement restorative materials. BMC Oral Health. 2022;22:1–7.
9. Jassal M, Mittal S, Tewari S. Clinical effectiveness of a resin-modified glass ionomer cement and a mild one-step self-etch adhesive applied actively and passively in noncarious cervical lesions: an 18-month clinical trial. Oper Dent. 2018;43:581–92.
10. Ghilotti J, Mayorga P, Sanz JL, Forner L, Llena C. Remineralizing ability of Resin Modified Glass ionomers (RMGICs): a systematic review. J Funct Biomater. 2023;14:421.
11. Kim H-J, Bae HE, Lee J-E, Park I-S, Kim H-G, Kwon J, et al. Effects of bioactive glass incorporation into glass ionomer cement on demineralized dentin. Sci Rep. 2021;11:7016.
12. Amend S, Boutsiouki C, Bekes K, Kloukos D, Lygidakis NN, Frankenberger R, et al. Clinical effectiveness of restorative materials for the restoration of carious primary teeth without pulp therapy: a systematic review. Eur Archives Pediatr Dentistry. 2022;23:727–59.
13. Park EY, Kang S. Current aspects and prospects of glass ionomer cements for clinical dentistry. Yeungnam Univ J Med. 2020;37:169–78.
14. Hamdy T. Polymerization shrinkage in contemporary resin-based dental composites: a review article. Egypt J Chem. 2021;64:3087–92.
15. Fronza BM, Lewis S, Shah PK, Barros MD, Giannini M, Stansbury JW. Modification of filler surface treatment of composite resins using alternative silanes and functional nanogels. Dent Mater. 2019;35:928–36.
16. Marichelvam MK, Kumar CL, Kandakodeeswaran K, Thangagiri B, Saxena KK, Kishore K et al. Investigation on mechanical properties of novel natural fiber-epoxy resin hybrid composites for engineering structural applications. Case Stud Constr Mater. 2023;19.
17. Hamdy TM. Evaluation of flexural strength, impact strength, and surface microhardness of self-cured acrylic resin reinforced with silver-doped carbon nanotubes. BMC Oral Health. 2024;24:151.
18. Hamdy TM, Saniour SH, Sherief MA, Zaki DY. Effect of incorporation of 20 wt% amorphous nano-hydroxyapatite fillers in poly methyl methacrylate composite on the compressive strength. Res J Pharm Biol Chem Sci. 2015;6.
19. Abdelraouf RM, Bayoumi RE, Hamdy TM. Influence of Incorporating 5% Weight Titanium Oxide Nanoparticles on Flexural Strength, Micro-Hardness, Surface Roughness and Water Sorption of Dental Self-Cured Acrylic Resin. Polym 2022, Vol 14, Page 3767. 2022;14:3767.
20. Hamdy TM. Evaluation of compressive strength, surface microhardness, solubility and antimicrobial effect of glass ionomer dental cement reinforced with silver doped carbon nanotube fillers. BMC Oral Health. 2023;23:1–9.
21. Abdelnabi A, Hamza NK, El-Borady OM, Hamdy TM. Effect of different formulations and application methods of coral calcium on its remineralization ability on carious enamel. Open Access Maced J Med Sci. 2020;8:94–9.
22. Nicholson JW, Sidhu SK, Czarnecka B. Enhancing the mechanical properties of glass-ionomer dental cements: a review. Materials. 2020;13.
23. Hamdy TM, Mousa SMA, Sherief MA. Effect of incorporation of lanthanum and cerium-doped hydroxyapatite on acrylic bone cement produced from phosphogypsum waste. Egypt J Chem. 2020;63:1823–32.
24. Hamdy TM, El-Korashy SA. Novel bioactive zinc phosphate dental cement with low irritation and enhanced microhardness. E-J Surf Sci Nanotechnol. 2018;16:431–5.
25. Birant S, Ozcan H, Koruyucu M, Seymen F. Assesment of the compressive strength of the current restorative materials. Pediatr Dent J. 2021;31:80–5.
26. Sharma A, Mishra P. Time-dependent variation in compressive strengths of three posterior esthetic restorative materials: an in vitro study. Int J Prosthodont Restor Dent. 2016;6:63–5.
27. Arya A, Grewal MS, Arya V, Choudhary E, Duhan J. Stress distribution of endodontically treated mandibular molars with varying amounts of tooth structure restored with direct composite resin with or without cuspal coverage: a 3D finite element analysis. J Conserv Dent. 2023;26:20–5.
28. Dawood SH, Kandil MM, El-Korashy DI. Effect of aging on compressive strength, Fluoride Release, Water Sorption, and solubility of ceramic-reinforced Glass ionomers: an in Vitro Study. J Contemp Dent. 2019;9:78–84.
29. Dathan C, Nair P, Kumar KCS. Flexural Strength is a critical property of Dental Materials-An overview. Acta Sci Dent Scienecs. 2023;7:99–103.
30. Garoushi S, Vallittu P, Lassila L. Hollow glass fibers in reinforcing glass ionomer cements. Dent Mater. 2017;33:e86–93.
31. Idrissi H, Al, Annamma LM, Sharaf D, Jaghsi A, Al, Abutayyem H. Comparative evaluation of Flexural Strength of four different types of Provisional Restoration materials: an in Vitro Pilot Study. Children. 2023;10:380.
32. Gokul S, Sc A, Kumar M. Effect of E-glass fibers with conventional heat activated PMMA Resin Flexural Strength and Fracture Toughness of Heat activated PMMA Resin. Ann Med Heal Sci Res. 2018;8:189–92.
33. Puska M, Zhang M, Matinlinna JP, Vallittu PK. Silane-treated E-Glass Fiber-Reinforced Telechelic Macromer-based polymer-matrix composites. Silicon. 2014;6:57–63.
34. Arun prakash VR, Rajadurai A. Inter laminar shear strength behavior of acid, base and silane treated E-glass fibre epoxy resin composites on drilling process. Def Technol. 2017;13:40–6.
35. Wawrzyńczak A, Kłos J, Nowak I, Czarnecka B. Surface studies on glass powders used in Commercial Glass-Ionomer Dental cements. Molecules. 2021;26:5279.
36. ISO 113581. International Organization for Standardization: ISO 9917-1:2007. Dentistry - Water-based cements - part 1. Int Organ Stand. 2015;10406–1:20.
37. American Society for Testing and Materials. ASTMC266-03: standard test method for time and setting ofhydraulic-cement paste by Gilmore needles. PhiladelphiaASTM. 2000;2010(C):1–4.
38. Chen S, Cai Y, Engqvist H, Xia W. Enhanced bioactivity of glass ionomer cement by incorporating calcium silicates. Biomatter. 2016;6:e1123842.
39. International Organization for Standardization. ISO 9917-2: Dentistry- water based cements-part 2: Resin-modified cements. Geneve. 2017.
40. ISO 20795-1. 2008(E) Dentistry — Base polymers — Part 1: Denture base polymers. 2008.
41. Fonseca RB, Kasuya AVB, Favarão IN, Naves LZ, Hoeppner MG. The influence of polymerization type and reinforcement method on flexural strength of acrylic resin. Sci World J. 2015;2015.
42. Fonseca RB, Favarão IN, Kasuya AVB, Abrão M, da Luz NFM, Naves LZ. Influence of Glass Fiber wt% and silanization on mechanical Flexural Strength of Reinforced acrylics. J Mater Sci Chem Eng. 2014;2:11–5.
43. Singer L, Bierbaum G, Kehl K, Bourauel C. Evaluation of the flexural strength, water sorption, and solubility of a glass ionomer dental cement modified using phytomedicine. Mater (Basel). 2020;13:1–14.
44. Pastila P, Lassila LVJ, Jokinen M, Vuorinen J, Vallittu PK, Mäntylä T. Effect of short-term water storage on the elastic properties of some dental restorative materials-A resonant ultrasound spectroscopy study. Dent Mater. 2007;23:878–84.
45. Gonulol N, Ozer S, Sen Tunc E. Water sorption, solubility, and color stability of giomer restoratives. J Esthet Restor Dent. 2015;27:300–6.
46. Malhotra S, Bhullar KK, Kaur S, Malhotra M, Kaur R, Handa A. Comparative evaluation of compressive strength and flexural strength of GC gold hybrid, GIC conventional and resin-modified glass-ionomer cement. J Pharm Bioallied Sci. 2022;14:S214–6.
47. Bonifácio CC, Kleverlaan CJ, Raggio DP, Werner A, De Carvalho RCR, Van Amerongen WE. Physical-mechanical properties of glass ionomer cements indicated for atraumatic restorative treatment. Aust Dent J. 2009;54:233–7.
48. Wang L, D'Alpino PHP, Lopes LG, Pereira JC. Mechanical properties of dental restorative materials: relative contribution of laboratory tests. J Appl Oral Sci. 2003;11:162–7.
49. Lohbauer U. Dental glass ionomer cements as permanent filling materials? -Properties, limitations and future trends. Mater (Basel). 2010;3:76–96.
50. Hussein F. Evaluation of Water Sorption and Solubility of Nano Titania Enriched Glass Ionomer Cement Considering the Storage Solution and Time. Open Dent J. 2022;16.
51. Vaz M, Joshi M, Shetty U, Ghadage M, Kadam N. Comparative evaluation of Sorption and solubility of three Dental Luting cements in two media: an in Vitro Study. World J Dent. 2023;14:118–21.
52. Choe Y-E, Kim Y-J, Jeon S-J, Ahn J-Y, Park J-H, Dashnyam K, et al. Investigating the mechanophysical and biological characteristics of therapeutic dental cement incorporating copper doped bioglass nanoparticles. Dent Mater. 2022;38:363–75.
53. Nicholson JW, Sidhu SK, Czarnecka B. Enhancing the mechanical properties of glass-ionomer dental cements: a review. Materials. 2020.
54. Garoushi SK, He J, Vallittu PK, Lassila LVJ. Effect of discontinuous glass fibers on mechanical properties of glass ionomer cement. Acta Biomater Odontol Scand. 2018;4:72–80.
55. Hammouda IM. Reinforcement of conventional glass-ionomer restorative material with short glass fibers. J Mech Behav Biomed Mater. 2009;2:73–81.
56. Sathishkumar TP, Satheeshkumar S, Naveen J. Glass fiber-reinforced polymer composites - a review. J Reinf Plast Compos. 2014;33:1258–75.
57. Cho K, Wang G, Raju R, Rajan G, Fang J, Stenzel MH, et al. Influence of Surface Treatment on the Interfacial and Mechanical properties of Short

S-Glass Fiber-Reinforced Dental composites. ACS Appl Mater Interfaces. 2019;11:32328–38.
58. Ralph C, Lemoine P, Summerscales J, Archer E, McIlhagger A. Relationships among the chemical, mechanical and geometrical properties of basalt fibers. Text Res J. 2019;89:3056–66.
59. Dionysopoulos D, Gerasimidou O, Papadopoulos C. Modifications of Glass Ionomer cements using nanotechnology: recent advances. Recent Prog Mater. 2022;4:1–1.
60. Alatawi RAS, Elsayed NH, Mohamed WS. Influence of hydroxyapatite nanoparticles on the properties of glass ionomer cement. J Mater Res Technol. 2019;8:344–9.
61. Mazzoli A, Moriconi G. Particle size, size distribution and morphological evaluation of glass fiber reinforced plastic (GRP) industrial by-product. Micron. 2014;67:169–78.
62. Memon IA, Jhatial AA, Sohu S, Lakhiar MT, Khaskheli ZH. Influence of Fibre length on the Behaviour of Polypropylene Fibre Reinforced Cement concrete. Civ Eng J. 2018;4:2124–31.
63. G PAFFENBARGER. American Dental Association specification 8 for Dental Zinc phosphate cement. J Am Dent Assoc Dent Cosm. 1937;24:2019–23.
64. Khajuria RR, Singh R, Barua P, Hajira N, Gupta N, Thakkar RR. Comparison of film thickness of two commercial brands of glass ionomer cement and one dual-cured composite: an in vitro study. J Contemp Dent Pract. 2017. https://doi.org/10.5005/jp-journals-10024-2104.
65. Khan AS, Azam MT, Khan M, Mian SA, Rehman IU. An update on glass fiber dental restorative composites: a systematic review. Mater Sci Eng C. 2015;47:26–39.
66. Tanaka CB, Ershad F, Ellakwa A, Kruzic JJ. Fiber reinforcement of a resin modified glass ionomer cement. Dent Mater. 2020;36:1516–23.
67. Gopinath A, Senthilkumar M, Babu A. Evaluation of Mechanical Properties and Microstructure of Polyester and Epoxy Resin Matrices Reinforced with Jute, E-glass and coconut Fiber. In: Materials Today: Proceedings. 2018. pp. 20092–103.
68. Alhotan A, Yates J, Zidan S, Haider J, Silikas N. Flexural strength and hardness of filler-reinforced pmma targeted for denture base application. Mater (Basel). 2021;14.
69. Oh D, Jang J, Jee J, Kwon Y, Im S, Han Z. Effects of fabric combinations on the quality of glass fiber reinforced polymer hull structures. Int J Nav Archit Ocean Eng. 2022;14:100462.
70. Nayak SY, Heckadka SS, Thomas LG, Baby A. Tensile and Flexural properties of chopped strand E-glass Fibre Mat Reinforced CNSL-Epoxy composites. MATEC Web Conf. 2018;144:2025.
71. Mohamed YS, El-Gamal H, Zaghloul MMY. Micro-hardness behavior of fiber reinforced thermosetting composites embedded with cellulose nanocrystals. Alexandria Eng J. 2018;57:4113–9.
72. Seshavenkat Naidu B, Krovvidi S. Fabrication of E-Glass Fibre Based Composite Material with Induced Particulate Additives. In: IOP Conference Series: Materials Science and Engineering. 2021.
73. Palmiyanto MH, Surojo E, Ariawan D, Imaduddin F. E-glass/kenaf fibre reinforced thermoset composites fiiled with MCC and immersion in a different fluid. Sci Rep. 2022;12:20332.
74. Murugan R, Yazid F, Nasruddin NS, Anuar NNM. Effects of Nanohydroxyapatite Incorporation into Glass Ionomer Cement (GIC). Minerals. 2021;12:9.
75. Beketova A, Tzanakakis E-GC, Vouvoudi E, Anastasiadis K, Rigos AE, Pandoleon P, et al. Zirconia nanoparticles as reinforcing agents for Contemporary Dental Luting cements: Physicochemical Properties and Shear Bond Strength to Monolithic Zirconia. Int J Mol Sci. 2023;24:2067.
76. Abed FM, Kotha SB, AlShukairi H, Almotawah FN, Alabdulaly RA, Mallineni SK. Effect of different concentrations of silver nanoparticles on the quality of the Chemical Bond of Glass Ionomer Cement Dentine in Primary Teeth. Front Bioeng Biotechnol. 2022;10:9.
77. Chaudhary S, Sinha AA, Showkat I. Comparative evaluation of compressive strength of conventional glass ionomer cement and glass ionomer cement modified with nano-particles. ~ 574 ~ Int J Appl Dent Sci. 2020;6:574–6.

Publisher's Note